DOI:10.11916/j.issn.1005-9113.17009

Theoretic Diffraction Research on the Order-Disorder Effect of Transition Metal in $Li(Ni_{1/3}Co_{1/3}Mn_{1/3})O_2$

Chunhui Cao[1,2], *Jian Zhang*[1*], *Chuanzheng Yang*[1] *and Baojia Xia*[1]

(*1.Shanghai Institute of Microsystem of Information Technology, Shanghai 200050, China;*
2.University of Chinese Academy of Sciences, Beijing 100049, China)

Abstract: After describing research status of super-structure for $Li(Ni_{1/3}Co_{1/3}Mn_{1/3})O_2$, diffraction patterns of $Li(Ni_{1/3}Co_{1/3}Mn_{1/3})O_2$ in different order parameters have been researched by Powder-cell program, including crystal structure, X-ray and neutron diffraction pattern, anomalous diffraction pattern and comparison of Ni Co Mn in different positions. The influence of order parameters on intensity of matrix and super-lattice diffraction lines has also been analyzed and the summarization and prospect have been made lastly.

Keywords: $Li(Ni_{1/3}Co_{1/3}Mn_{1/3})O_2$; order-disorder; diffraction

CLC number: O721 **Document code**: A **Article ID**: 1005-9113(2018)06-0078-12

1 Introduction

Due to its high cost and toxicity, commercial cathode material $LiCoO_2$ in lithium ion batteries is gradually replaced by $Li(Ni, Co, Mn)O_2$, among which $Li(Ni_{1/3}Co_{1/3}Mn_{1/3})O_2$ is the most competitive for its over-all properties[1-4]. All of these cathode materials have a rhomboidal structure with trigonal symmetry (space group: R-3m, No.166), which is layer-structural with α-$NaFeO_2$. Usually, transition metal ions Me (Ni, Co, Mn) are located in octahedral 3*b* (0 0 1/2) sites and oxygen anions are in a cubic close-packing, occupying the 6*c*(0 0 *z*) sites. Lithium cations reside at Wyckoff 3*a*(0 0 0) sites, represented as $[Li]_{3a}[Me]_{3b}[O_2]_{6c}$. In addition, there are three symmetry operations in this structure, including (0,0,0), (1/3,2/3,2/3), (2/3,1/3,1/3).

Since the discovery of $Li(Ni_{1/3}Co_{1/3}Mn_{1/3})O_2$, the arrangement of transition metal in 3*b* is the key point of contention[5-10]. At present, there are three supposed models for it. The first model, as illustrated in Fig.1 (a), consists of $[Co_{1/3}Ni_{1/3}Mn_{1/3}]O_2$ slabs of the $[\sqrt{3}\times\sqrt{3}]$R30°-type super-lattice in Wood's notation based on basal net in triangular lattice of sites. The second model (Fig.1(b)) consists of CoO_2, NiO_2 and MnO_2 slabs piled up regularly[11]. In the third model, Ni, Co and Mn are randomly located in 3*b*, i.e. disorderly O3 structure.

The formation energy of the super-lattice model calculated by Koyama et al.[11] was −0.17 eV per formula unit, and that of stacking model was +0.06 eV. So it is more possible that the super-lattice model exists, which restricts the volume change of cathode between charging and discharging and improves cycling life due to the stable lattice structure. Through XRD refinement, Yabuuchi et al.[11] found that the $[\sqrt{3}\times\sqrt{3}]$R30°-type super-lattice fit well with the actual diffraction spectral, belonged to $P3_112$, not simple $R\bar{3}m$. Furthermore, electron diffraction study indicated that there exited the $[\sqrt{3}\times\sqrt{3}]$R30°-type super-lattice in crystal zone[11.0], as shown in Fig.2 (The reflection indices were based on $R\bar{3}m$ in Hexagonal).

Although the arrangement of inner atom in $Li(Ni_{1/3}Co_{1/3}Mn_{1/3})O_2$ can be verified by calculation and detection, it cannot be proved that this material has the completely orderly arrangement[13-17] in Fig.1(a). Whitfield[18] studied the structure of $Li(Ni_{1/3}Co_{1/3}Mn_{1/3})O_2$ by neutron (as shown in Fig.3) and anomalous dispersion powder diffraction and found a random distribution of Mn, Ni, and Co over the $R\bar{3}m$ 3*b* sites. Rietveld analyses (as shown in Table 1) indicated that about 2% nickel migrated from

Received 2017-01-19.
Sponsored by the National Key Research and Development Program (Grant No.2016YFB0100500).
* Corresponding author. E-mail: zjskycn@163.com.

3*b* site to 3*a* site due to the similar atomic radius of Ni^{2+} (r_{Ni2+} = 0.69 Å) and Li^+ (r_{Li+} = 0.76 Å), which was also called cation disorder. The more Ni^{2+} cations in Li^+ layer, the harder deintercalate-intercalate of Li^+, so the electrochemical performances became worse.

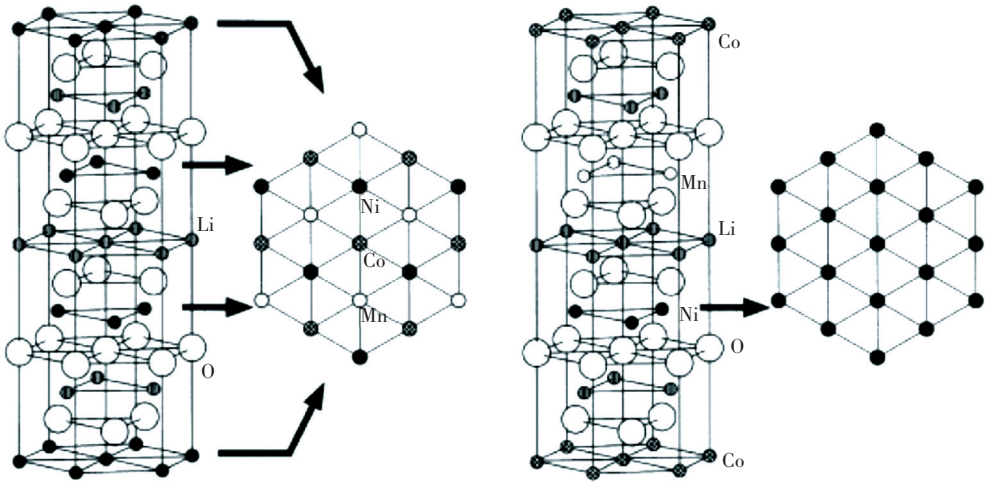

(a) Superlattice of [$\sqrt{3}\times\sqrt{3}$]R30° (b) Piled-up

Fig.1 Structural model of Li($Ni_{1/3}Co_{1/3}Mn_{1/3}$)O_2 (Reprinted with permission from Koyama et al.[11] Copyright 2003, Elsevier)

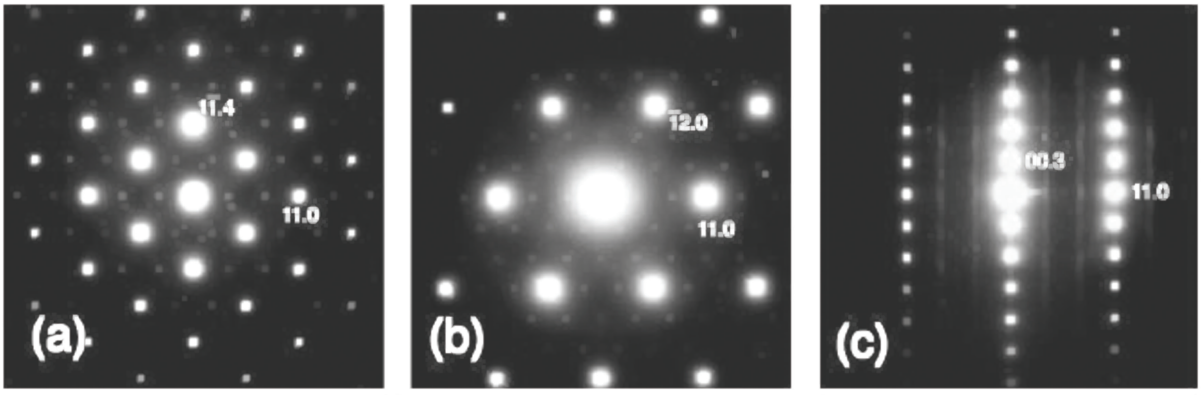

(a) [22.1] (b) [00.1] (c) [11.0]

Fig.2 Electron diffraction patterns of Li($Ni_{1/3}Co_{1/3}Mn_{1/3}$)O_2 (Reprinted with permission from Yabuuchi et al.[12] Copyright 2005, the Electrochemical Society)

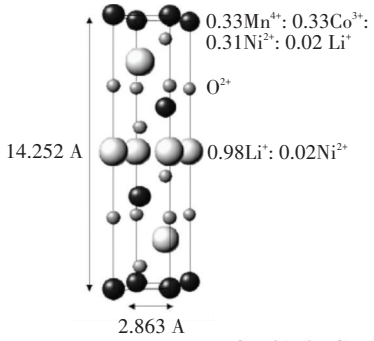

Fig.3 The crystal structure of Li($Ni_{1/3}Co_{1/3}Mn_{1/3}$)O_2 (Reprinted with permission from Whitfield et al.[18] Copyright 2005, Elsevier)

Table 1 The occupation of atoms for Li($Ni_{1/3}Co_{1/3}Mn_{1/3}$)O_2 after refinement(Data from whitfield et al.[18])

Ion	Position	*x*	*y*	*z*	Occupancy	*B*(Temp.)
Li^+	3*a*	0	0	0	0.978 1	1.236
Ni^{2+}	3*a*	0	0	0	0.021 3	0.429
Li^+	3*b*	0	0	0.500	0.024 2	1.236
Ni^{2+}	3*b*	0	0	0.500	0.309 2	0.429
Co^{3+}	3*b*	0	0	0.500	0.332 0	0.429
Mn^{4+}	3*b*	0	0	0.500	0.334 6	0.429
O^{2-}	6*c*	0	0	0.259	1.000 0	0.663

The super lattice diffraction lines may appear after ordering treatment the order degree has an effect on the diffraction intensity of super lattice line; sometimes the super lattice diffraction lines do not appear but the diffraction intensity of matrix diffraction lines change[19-22]. So we can calculate the order degree by diffraction intensity data, which depends on the crystal structure[23]. In this paper Powder-cell was used to simulate diffraction patterns and intensity of the super and matrix lattices.

2 Crystal Structure

It was supposed that theorder degree S, was 0, 0.5 and 1. Space group was No. 166, $R\bar{3}m$, a = 2.963, c = 14.252, the atom positions[24] are shown in Table 2. When S was 0, Ni, Co and Mn were randomly occupied in (0,0,1/2), (1/3,2/3,7/6) and (2/3,1/3,5/6), whose occupancy(SOF) were 1/3. When S was 1, Ni, Co and Mn were orderly occupied respectively in (0,0,1/2), (1/3,2/3,7/6) and (2/3,1/3,5/6), whose SOF were 1.0. When S was 0.5, it became complicated. Ni, Co and Mn were occupied in (0,0,1/2), (1/3,2/3,7/6) and (2/3, 1/3,5/6) by order degree of 0.5. At the same time, they were occupied in 3b site by SOF = 0.5×0.333 = 1/6. The crystal structure model was illustrated in Fig.4.

Table 2 The atom positions in different order degree

S	Element	Z	Ion	Wyck	x	y	z	SOF	B (Temp.)
	Li	3	Li	3a	0	0	0	1.00	1.236
	Ni	28	Ni	3b	0	0	1/2	1/3	0.429
0.0	Co	27	Co	3b	0	0	1/2	1/3	0.429
	Mn	25	Mn	3b	0	0	1/2	1/3	0.429
	O	8	O	6c	0	0	1/4	1.00	0.663
	Li	3	Li	3a	0	0	0	1.00	1.236
	Ni	28	Ni		0	0	1/2	1/2	0.429
	Co	27	Co		1/3	2/3	7/6	1/2	0.429
0.5	Mn	25	Mn		2/3	1/3	5/6	1/2	0.429
	Ni	28	Ni	3b	0	0	1/2	1/6	0.429
	Co	27	Co	3b	0	0	1/2	1/6	0.429
	Mn	25	Mn	3b	0	0	1/2	1/6	0.429
	O	8	O	6c	0	0	1/4	1.00	0.663
	Li	3	Li	3a	0	0	0	1.00	1.236
	Ni	28	Ni	3b	0	0	0.50	1.00	0.429
1.0	Co	27	Co	3b	1/3	2/3	7/6	1.00	0.429
	Mn	25	Mn	3b	2/3	1/3	5/6	1.00	0.429
	O	8	O	6c	0	0	1/4	1.00	0.663

3 X-ray and Neutron Diffraction Pattern

Figs.5 and 6 show the diffraction patterns of X-ray and neutron at different S, and the specific data is listed in Table 3. As we can infer from the comparison data, there are obvious difference between the XRD pattern and neutron diffraction pattern. Three strength lines are distinct, the first strength line is different. The second strength lines decrease with the increase of S, but the third lines are almost constant. This is because that the scattering factors of Ni, Co, Mn have little difference for X-ray, while the difference for neutron is much larger. So the problem of order occupying position of neighboring atom is often studied by neutron diffraction[7].

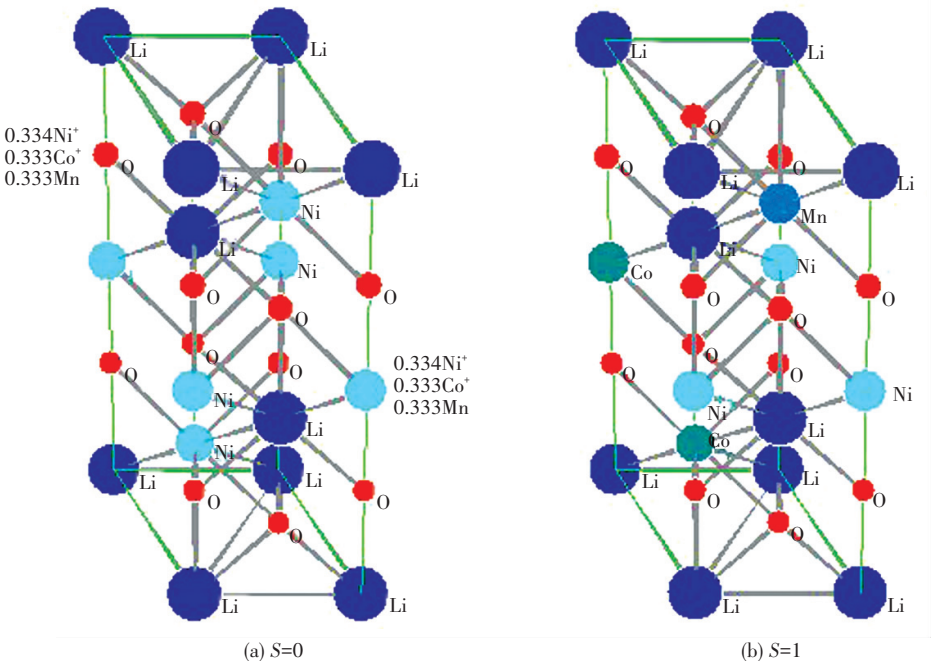

Fig.4 The crystal structure model of $Li(Ni_{1/3}Co_{1/3}Mn_{1/3})O_2$ when S was 0 and 1

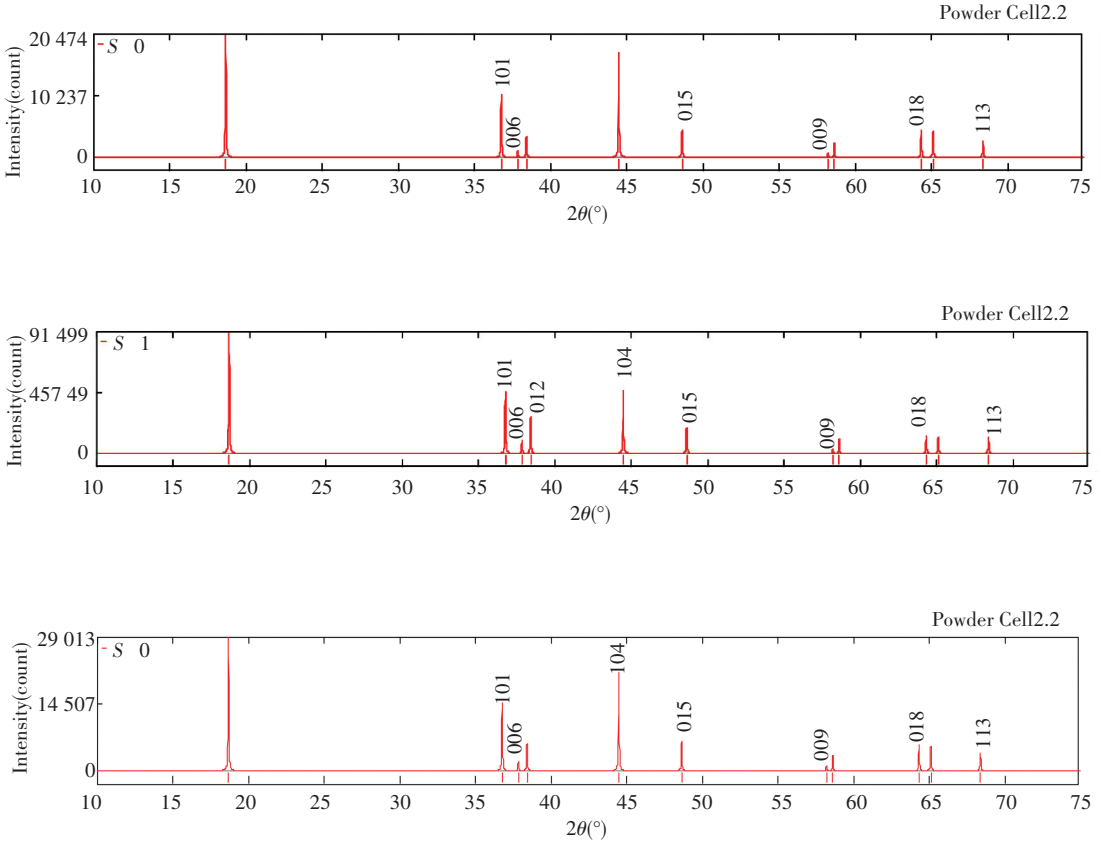

Fig.5 XRD patterns of $Li(Ni_{1/3}Co_{1/3}Mn_{1/3})O_2$ at $S=0$, 0.5 and 1 ($\lambda=1.540\ 6$ Å)

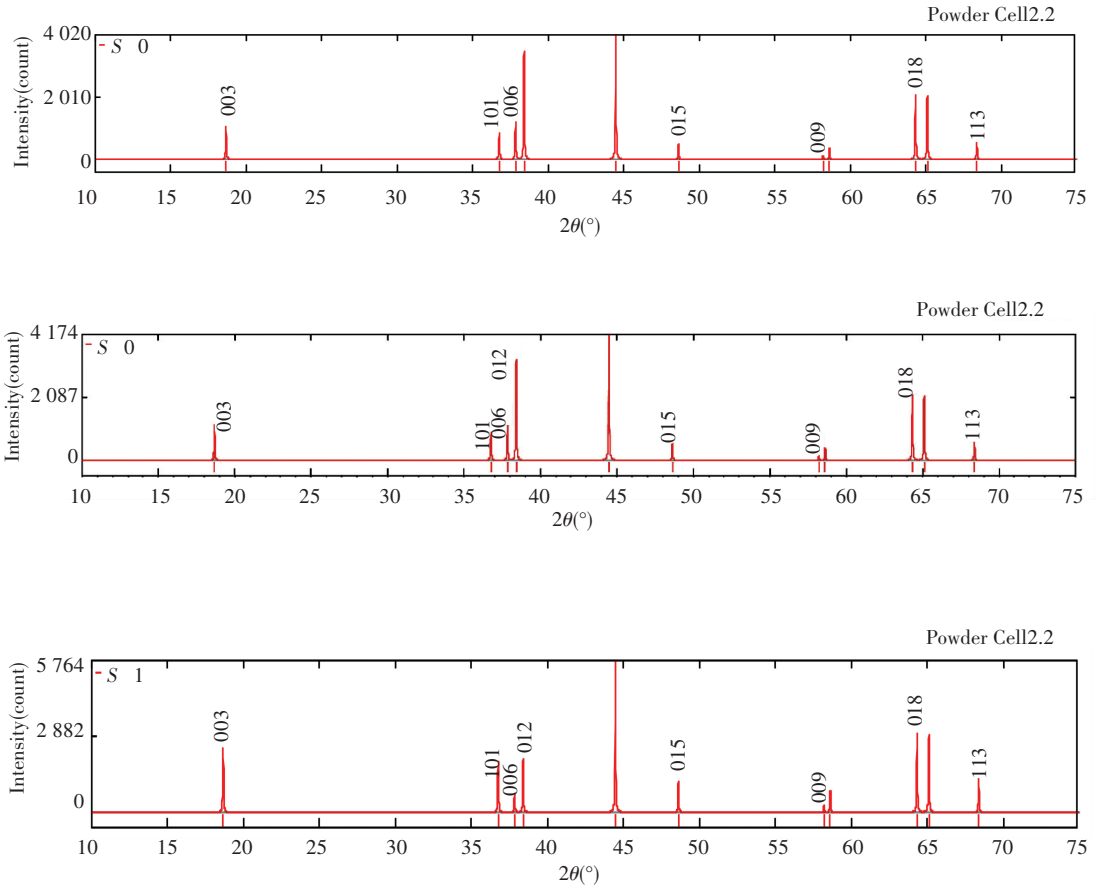

Fig.6 Neutron diffraction patterns of $Li(Ni_{1/3}Co_{1/3}Mn_{1/3})O_2$ at $S=0$, 0.5 and 1 ($\lambda=1.540\ 6$ Å)

Table 3 Relative diffraction intensity of X-ray and neutron at different S ($\lambda=1.540\ 6$ Å)

hkl	*d* (Å)	2*θ* (°)	Relative intensity (%)					
			S = 0		*S* = 0.5		*S* = 1.0	
			X-ray	Neutron	X-ray	Neutron	X−ray	Neutron
003	4.750 670	18.663 0	**100.00**	26.69	**100.00**	28.29	**100.00**	42.42
101	2.442 740	36.763 0	**51.14**	21.04	**51.08**	22.31	**50.78**	33.65
006	2.375 330	37.845 0	5.66	29.82	6.91	27.39	10.21	11.93
012	2.341 730	38.409 0	16.38	**89.90**	19.97	**79.83**	29.41	34.74
104	2.035 160	44.481 0	**84.84**	**100.00**	**73.82**	**100.00**	**51.24**	**100.00**
015	1.887 073	48.632 0	21.47	12.30	21.46	13.06	21.24	19.80
009	1.583 560	58.213 0	3.89	2.94	3.89	3.12	2.87	4.76
107	1.573 480	58.622 0	11.40	8.71	11.39	9.26	11.32	14.10
018	1.446 770	64.339 0	22.18	**51.93**	19.48	**51.93**	13.90	**52.02**
110	1.431 500	65.110 0	21.20	50.91	18.64	50.93	13.32	**51.02**
113	1.370 630	68.138 9	13.32	13.31	13.32	14.13	13.22	21.69

4 Comparison of Ni, Co, Mn Occupied in Different Positions

The diffraction data was listed in Table 4 when $S=1$ and Ni, Co and Mn occupied in different position. It is known from the comparison that three strength distribution and relative intensities are the same and their structure amplitudes are similar.

Table 4 Diffraction data when Ni, Co and Mn occupy in different positions ($\lambda=1.540\ 6$ Å)

hkl	*d* (Å)	2θ (°)	Ni 0 0 1/2 Co 1/3 2/3 7/6 Mn 2/3 1/3 5/6		Co 0 0 1/2 Mn 1/3 2/3 7/6 Ni 2/3 1/3 5/6		Mn 0 0 1/2 Ni 1/3 2/3 7/6 O 2/3 1/3 5/6	
			$I./I_0$ (%)	$\lvert F(hkl)\rvert$	$I./I_0$ (%)	$\lvert F(hkl)\rvert$	$I./I_0$ (%)	$\lvert F(hkl)\rvert$
003	4.750 67	18.663	**100.00**	**131.94**	**100.00**	**125.55**	**100.00**	**135.13**
101	2.442 74	36.893	**58.25**	**119.22**	**57.93**	**113.12**	**58.46**	**122.31**
006	2.375 33	37.845	11.80	95.94	11.42	89.88	11.98	99.02
012	2.341 73	38.536	32.85	93.96	31.76	87.91	33.41	97.04
104	2.035 16	44.592	**56.44**	**145.09**	**57.39**	**139.22**	**56.06**	**148.09**
015	1.870 73	48.735	27.15	111.32	26.97	105.58	27.27	114.27
009	1.583 56	58.213	5.33	104.76	5.29	99.37	5.35	107.57
107	1.573 48	58.713	10.45	85.38	10.13	80.00	10.62	88.18
018	1.446 77	64.425	14.94	113.20	15.04	108.06	14.93	115.90
110	1.431 50	65.366	14.81	114.18	14.93	109.06	14.79	115.86
113	1.370 63	68.640	13.65	81.62	13.29	75.65	13.86	84.24

5 Anomalous X-ray Diffraction Pattern

The anomalous diffraction is a diffraction experiment one using the radiation of some element's absorbing wavelength as incident ray, called as the anomalous scattering or anomalous diffraction, which is also called diffraction of choosing elements.

When there is anomalous diffraction, the total atomic scattering factor is given by:

$$f_{(S,\lambda)}=f_{0(S)}+f'_{(S,\lambda)}+\mathrm{i}f''_{(S,\lambda)} \tag{1}$$

where f' and f'' are the real and imaginary parts of anomalous diffraction correction, f' and f_0 have the opposite phases, the phase of f'' is 90°. And f is:

$$f=\sqrt{(f_0+f')^2+(f'')^2} \tag{2a}$$

The approximate form is:

$$f=f_0+f'+\frac{1}{2}\frac{(f'')^2}{f_0+f'} \tag{2b}$$

The effects of anomalous diffraction on total scattering factor are as follows:

1) Anomalous diffraction can be ignored when the incident ray's wavelength is far from absorbing limit;

2) Near the absorption limit, anomalous scattering correction is quite large and increases with the scattering angle;

3) When the incident ray's wavelength is equal to absorption limit, anomalous diffraction can play a dominant position at high diffraction angles;

4) Anomalous diffraction correction is related to the atom number of the scattered due to different element has different absorbing limit.

So we can study the long range order of neighboring atoms by anomalous diffraction in principle. As seen from Table 5, the position of diffraction lines increases with the wavelength and moves to the high angle, while the relative intensity has no change. It seems that anomalous diffraction has no effect, but actually possible cause is that Powdercell could not carry out the correction of the anomalous scattering.

Table 5 Comparison of anomalous diffraction data at $S=1$

hkl	d (Å)	2θ (°)				Relative intensity (%)			
		Ni absorbing limit is 1.488 01	CuKα radiation is 1.540 56	Co absorbing limit is1.608 2	Mn absorbing limit is 1.896 4	Ni absorbing limit is 1.488 1	CuKα radiation is 1.540 56	Co absorbing limit is 1.608 2	Mn absorbing limit is 1.896 4
003	4.750 67	18.021	18.663	19.489	23.027	**100.00**	**100.00**	**100.00**	**100.00**
101	2.442 74	35.592	36.893	38.573	45.846	**51.12**	**50.78**	**50.33**	**48.35**
006	2.375 33	36.508	37.845	39.572	47.055	10.28	10.21	10.11	9.69
012	2.341 73	37.171	38.536	40.295	47.931	29.63	29.41	29.12	27.87
104	2.035 16	42.994	44.592	46.660	55.682	**51.76**	**51.24**	**50.58**	**47.84**
015	1.870 73	46.971	48.735	51.021	61.046	21.58	21.24	21.01	19.79
009	1.583 56	56.049	58.213	61.030	73.566	3.92	3.87	3.80	3.64
107	1.573 48	56.527	58.713	61.559	74.238	11.48	11.32	11.13	10.67
018	1.446 77	61.980	64.425	67.618	82.019	14.08	13.90	13.71	13.65
110	1.431 50	62.877	65.366	68.620	83.321	13.49	13.32	13.14	13.18
113	1.370 63	65.993	68.640	72.106	87.901	13.36	13.22	13.09	13.62

6 Influence of Order Degree on Intensity of Matrix Diffraction

The analysis shows that the order of Ni, Co and Mn in the 3*b* position has little effect on the matrix diffraction relative intensity for both the conventional and anomalous X-ray diffraction.

Under symmetric Bragg reflection geometry condition in the X-ray powder diffraction, the relative integral intensity for single-phase can be expressed as follows:

$$I_{hkl} = P_{hkl} \mid F_{hkl} \mid^2 \frac{1 + \cos^2 2\theta_{hkl}}{\sin^2\theta_{hkl}\cos\theta_{hkl}} \tag{3}$$

where P_{hkl} is the multiplicity factor of crystal plane (hkl), F_{hkl} is structure factor, the last is angle factor. The formula of structure factor is:

$$F_{hkl} = \sum_{j=1}^{n} f_j e^{2\pi i(hx_j+ky_j+lz_j)} = \sum_{j=1}^{n} f_j [\cos 2\pi(hx_j + ky_j + lz_j) + i\sin 2\pi(hx_j + ky_j + lz_j)] \tag{4}$$

where f_j is the scattering factor of j atom. x_j, y_j, z_j is the coordinate of j atom. Summation is for all atoms in single cell. Specifically for $Li(Ni_{1/3}Co_{1/3}Mn_{1/3})O_2$, they contain 3 Li atoms, 3 transition metal atoms and 6 oxygen atoms. The position parameters of main diffraction lines are listed in Table 6.

Suppose f_{3a}, f_{3b}, f_{6c} are the atom scattering factor of atoms on 3*a*, 3*b* and 6*c* position, then we get the following formula for $Li(Ni_{1/3}Co_{1/3}Mn_{1/3})O_2$:

$$\begin{cases} f_{3a} = f_{(3a)1} + f_{(3a)2} + f_{(3a)3} = 3f_{Li} \\ f_{6c} = f_{(6c)1} + f_{(6c)2} + \cdots\cdots + f_{(3c)6} = 6f_o \end{cases} \tag{5}$$

f_{3b} is complicated, when $S = 0$,

$$f_{3b} = \frac{1}{3}(f_{Ni} + f_{Co} + f_{Mn}) \times 3 \tag{6}$$

when $S = 1$

$$f_{3b} = f_{Ni} + f_{Co} + f_{Mn} \tag{7}$$

when $0 < S < 1$

$$f_{3b} = S \times (f_{Ni} + f_{Co} + f_{Mn}) + (1 - S) \times \frac{1}{3}(f_{Ni} + f_{Co} + {}_{Mn}) \times 3 \tag{8}$$

Eq.(8) shows that, when $0 < S < 1$, atomic scattering factor of 3*b* position includes two parts. The first item describes the orderly occupying part, while the second item describes contribution of randomly occupied atoms remaining after orderly occupying. f_{Li}, f_{Ni}, f_{Co}, f_{Mn}, f_o are the scattering factor of Li, Ni, Co, Mn and O atoms respectively. They are all the functions of $(\sin\theta)/\lambda$ and decrease with $(\sin\theta)/\lambda$ increasing. For the same diffraction pattern, λ is constant, which means atom scattering factor decreases with 2θ increasing.

Similarly, the diffraction angle factor $(1+\cos^2 2\theta_{hkl})/(\sin^2\theta_{hkl}\cos\theta_{hkl})$ decreases with 2θ increasing. The specific values can be calculated or obtained from professional books.

Thus, main characters of each diffraction lines of $Li(Ni_{1/3}Co_{1/3}Mn_{1/3})O_2$ can be summarized as follows:

(1) Considering the contribution of oxygen on 6*c* position to diffraction intensity, it can be divided into:

No contribution: 003, 101, 015, 009, 107, 018, 113;

The addition: 104, 110;

The subtraction: 006, 012.

Table 6 Atom position parameters of $R\bar{3}m$(No.166)

Position	Atom coordinate	Position-parameters $\cos 2\pi(hx_j + ky_j + lz_j) + i\sin 2\pi(hx_j + ky_j + lz_j)$										
		003	101	006	012	104	015	009	107	018	110	113
		100	40	12	15	95	18	9	20	25	25	13
3*a*	0 0 0	+1	+1	+1	+1	+1	+1	+1	+1	+1	+1	+1
	2/3 1/3 1/3	+1	+1	+1	+1	+1	+1	+1	+1	+1	+1	+1
	1/3 2/3 2/3	+1	+1	+1	+1	+1	+1	+1	+1	+1	+1	+1
	$\sum$	+3	+3	+3	+3	+3	+3	+3	+3	+3	+3	+3
3*b*	0 0 1/2	−1	−1	+1	+1	+1	−1	−1	−1	+1	+1	−1
	2/3 1/3 5/6	−1	−1	+1	+1	+1	−1	−1	−1	+1	+1	−1
	1/3 2/3 7/6	−1	−1	+1	+1	+1	−1	−1	−1	+1	+1	−1
	$\sum$	−3	−3	+3	+3	+3	−3	−3	−3	+3	+3	−3
6*c*	0 0 1/4	−i	+i	−1	−1	+1	−i	−i	+i	−i	+1	−i
	2/3 1/3 7/12	−i	+i	−1	−1	+1	−i	−i	+i	−i	+1	−i
	+/3 2/3 11/12	−i	+i	−1	−1	+1	−i	−i	+i	−i	+1	−i
	0+ 0−1/4	+i	−i	−1	−1	+1	+i	+i	−i	+i	+1	+i
	2/3 1/3 1/12	+i	−i	−1	−1	+1	+i	+i	−i	+i	+1	+i
	1/3 2/3 5/12	+i	−i	−1	−1	+1	+i	+i	−i	+i	+1	+i
	$\sum$	0	0	−6	−6	+6	0	0	0	0	+6	0
Contribution of 3*a* and 3*b*		−	−	+	+	+	−	−	−	+	+	−

(2) Considering the contribution of atoms on 3*a* and 3*b*, it can be divided into:

The addition: 006, 012, 104, 110, 018;

The subtraction: 003, 101, 015, 009, 107, 113.

(3) The "addition" and "subtraction" relationship reveals a very important rule. Take 003, 101 and 104 as examples, F_{hkl} is:

$$\begin{cases} F_{003} = 3f_{\mathrm{Li}}^{003} - S \times (f_{\mathrm{Ni}}^{003} + f_{\mathrm{Co}}^{003} + f_{\mathrm{Mn}}^{003}) - (1 - S) \times \dfrac{1}{3}(f_{\mathrm{Ni}}^{003} + f_{\mathrm{Co}}^{003} + f_{\mathrm{Mn}}^{003}) \times 3 \\ F_{101} = 3f_{\mathrm{Li}}^{101} - S \times (f_{\mathrm{Ni}}^{101} + f_{\mathrm{Co}}^{101} + f_{\mathrm{Mn}}^{101}) - (1 - S) \times \dfrac{1}{3}(f_{\mathrm{Ni}}^{101} + f_{\mathrm{Co}}^{101} + f_{\mathrm{Mn}}^{101}) \times 3 \\ F_{104} = 3f_{\mathrm{Li}}^{104} + S \times (f_{\mathrm{Ni}}^{104} + f_{\mathrm{Co}}^{104} + f_{\mathrm{Mn}}^{104}) + (1 - S) \times \dfrac{1}{3}(f_{\mathrm{Ni}}^{104} + f_{\mathrm{Co}}^{104} + f_{\mathrm{Mn}}^{104}) \times 3 + 6f_{\mathrm{O}}^{104} \end{cases} \tag{9}$$

The diffraction line 104 is stronger than 101. The first part in the formula is the contribution of Li atoms; the second part is the contribution of orderly Ni, Co, Mn on 3*b*; the third part is the contribution of randomly Ni, Co, Mn on 3*b*; the fourth part is the contribution of oxygen on 6*c*. It can be inferred from Eq.(9) that the contribution of 3*a* and 3*b* to 003 and 101 is subtraction, for both 003 and 101 oxygen have not contribution. While contribution of 3*a* and 3*b* to 104 is addition.

With $S = 0, 0.2, 0.4, 0.6, 0.8, 1.0$, the relative intensity of the calculation results (as shown in Table 8) and analysis results show that there is no influence of order degree on diffraction intensity matrix lines. In other words, the diffraction intensity of matrix lines has no relationship with order and disorder in the 3*b* site. Therefore the order degree, S, cannot be solved from the diffraction data of matrix lines.

7 Influence of Order Degree on Intensity of Super-lattice Diffraction Line

It is known from the above research that the ordering on 3*b* positions does not show diffraction lines of super-lattice for $Li(Ni_{1/3}Co_{1/3}Mn_{1/3})O_2$ belong to the No.166 space group structure. In order to prove whether it is right, the author has made a simulated study diffraction patterns of the classic $AuCu_3$ super structure. The result shows that only when the use of crystallographic position are the same, but space group (extinction rule) is different, (No. 225, Fm - 3m and No. 221, Pm - 3m), diffraction pattern calculated can show the super-lattice lines. It can derive from his conclusion that above simulated diffraction patterns using No. 166 space group do not appear super-lattice lines cannot prove that the diffraction pattern of $Li(Ni_{1/3}Co_{1/3}Mn_{1/3})O_2$ with super-structure cannot appear super lattice lines.

In the rhombohedral system with space group (No. 143 - No. 167) was not found corresponding space group which x, y, z coordinates are the same with (3*b*) positions in No. 166 space group and the extinction conditions are different. That No.166 after (3*b*) ordering has symmetry of $P3_112$ (No.151)[18] is questionable, because x, y, z coordinates of atoms are obviously different and extinction rule is similar between No.151 and No.166 space group.

To this end, wecalculated the crystallographic position parameters of space group No. 166 may appear the super-lattice lines: 001, 002, 004, 111, as shown in Table 7.

Table 7 Position parameters of space group No.166

Position	Atom coordinate *hkl*	Parameters $\cos 2\pi(hx_j + ky_j + lz_j) + i\sin 2\pi(hx_j + ky_j + lz_j)$			
		001	002	004	111
3*a*	0 0 0	1	1	1	1
	2/3 1/3 1/3	-0.5+0.866i	-0.5-0.866i	-0.5+0.866i	-05+0.866i
	1/3 2/3 2/3	-0.5-0.866i	-0.5+0.866i	-0.5-0.866i	-0.5-0.866i
	$\sum$	0	0	0	**0**
3*b*	0 0 1/2	-1	1	1	-1
	2/3 1/3 5/6	0.5-0.866i	-0.5-0.866i	-0.5+0.866i	0.5-0.866i
	1/3 2/3 7/6	0.5+0.866i	-0.5+0.866i	-0.5-0.866i	0.5+0.866i
	$\sum$	0	0	0	**0**
6*c*	0 0 1/4	i	-1	1	i
	2/3 1/3 7/12	-0.866-0.5i	0.5+0.866i	-0.5+0.866i	-0.866-0.5i
	1/3 2/3 11/12	0.866-0.5i	0.5-0.866i	-0.5-0.866i	0.866-0.5i
	0 0 - 1/4	-i	-1	1	-i
	2/3 1/3 1/12	0.866+0.5i	0.5+0.866i	-0.5+0.866i	0.866+0.5i
	1/3 2/3 5/12	-0.866+0.5i	0.5-0.866i	-0.5-0.866i	-0.866+0.5i
	$\sum$	0	0	0	0

We can conclude from analysis of Table 7:

(1) The 3*a* and 6*c* position atoms are no contribution to the diffraction intensity of 001, 002, 004 and 111.

(2) 3*b* position atoms contribution to the diffraction intensity are more complex; when disordered ($S = 0$) occupation, the atomic scattering factors for each position are equal to ($f_{Ni} + f_{Co} +$

$f_{Mn})/3$ the same, such as, factor scatter factor for each position, the contribution of three position is equal to zero; when totally ordered ($S = 1$) occupation, the scattering factors of three position are different, the contribution of three positions is not zero, then the super-lattice lines can appear; and the larger the difference of atomic scattering factor between the three positions is, the stronger super-lattice line is. Therefore, using the anomalous diffraction techniques or/and neutron diffraction is beneficial to studying a super-lattice structure.

(3) When $0 < S < 1$, structure factor is divided into two parts, ordered partials have contributed to intensity and the remaining disorder part has no contribution to intensity.

The effect of order degree on the diffraction intensity has calculated using the data given in Table 8, because 104 and 111 almost overlap, so only for four diffraction of 002, 003, 004, 101 was calculated. The results are given in Table 9.

We can see from analysis of Table 9:

(1) The matrix diffraction intensity does not change with S, in other words, the diffraction intensity of matrix line is not influenced by S;

(2) Diffraction intensity of super-lattice lines increases with the increase of S, which can solve an order degree, S, according to the intensity data super-lattice diffraction lines or super-lattice and matrix diffraction lines.

(3) The relative intensity of super-lattice lines is very weak, even $S = 1$, the relative intensity of 002 and 004 super two points front is only 0.225% and 0.043%. So the general diffraction experiment is very difficult to detect the super-lattice lines.

Table 8 The relative parameters of several matrix and super-lattice lines

hkl	Multi factor	*D*	2θ	Angle factor	sinθ/λ	f_{Li}	f_{Ni}	f_{Co}	f_{Mn}	f_O
001	2	14.252 00	6.196	680.900	0.035		27.631	26.538	24.149	
002	2	7.126 00	12.412	168.500	0.070		26.638	25.664	24.271	
003	2	4.750 67	18.663	73.499	0.105	2.215	25.600	24.650	22.570	7.250
004	2	3.563 00	24.970	39.820	0.140		23.008	22.970	21.142	
101	6	2.442 74	36.893	17.150	0.205	1.741	21.370	20.540	19.000	
104	6	2.035 16	44.592	11.310	0.246	1.627	19.590	18.810	17.359	4.814
111	6	2.028 80	44.627	11.310	0.246		19.590	18.810	17.359	

Table 9 Calculated intensity and relative intensity of several matrix and super-lattice lines and influence of order degree

S	Intensity				Relative intensity			
	002	003	004	101	002	003	004	101
0.0	0	635 262.963	0	321 050.875	0	100.00	0	50.54
0.2	18.164 0	635 262.963	10.910 0	321 050.875	0.002 9	100.00	0.001 7	50.54
0.4	228.926 0	635 262.963	43.476 0	321 050.875	0.036 0	100.00	0.006 8	50.54
0.6	515.106 3	635 262.963	97.831 4	321 050.875	0.081 1	100.00	0.015 4	50.54
0.8	1 216.302 1	635 262.963	173.793 2	321 050.875	0.191 5	100.00	0.027 4	50.54
1.0	1 431.104 0	635 262.963	271.747 0	321 050.875	0.225 3	100.00	0.042 8	50.54

8 Conclusion and Prospect

For Li ($Ni_{1/3}Co_{1/3}Mn_{1/3}$)O_2, when Ni, Co, Mn ordered occupied in 3*b*, diffraction intensity of the matrix lines is not influenced by order degree S; but the diffraction intensity of super-lattice lines increase with the order degree. Theoretically, one can solve an ordering degree, S, according to the intensity data super-lattice diffraction lines or super-lattice and matrix diffraction lines, but it is very difficult because diffraction intensity of the super-lattice lines is very

weak, in general diffraction experiments.

Therefore, whether orderly occupying is existed in 3*b* of $Li(Ni_{1/3}Co_{1/3}Mn_{1/3})O_2$ and forms of super structure still need further study in the following aspects:

1) To explore the optimal process of ordering treatment for $Li(Ni_{1/3}Co_{1/3}Mn_{1/3})O_2$ material under the appropriate medium temperature;

2) To enhance the detection ability of diffraction experiment, use strong X-ray source, such as synchrotron radiation X-ray source, use high efficient detector, super fine experimental operation, such as slow speed scan and anomalous diffraction techniques or/and the neutron diffraction technique;

3) According to the relationship between diffraction intensity increases with the order degree increases, to determine the order degree of material; establish the relationship among ordering treatment process, order degree and materials (battery) performance.

References

[1] Li D, Zhang H Z, Wang C W, et al. New structurally integrated layered-spinel lithium-cobalt-manganese-oxide composite cathode materials for lithium-ion batteries. Journal of Alloys and Compounds, 2017, 696: 276-289. DOI: 10.1016/j.jallcom.2016.11.246.

[2] Zou Y H, Yang X F, Lv C X, et al. Multishelled Ni-Rich $Li(Ni_xCo_yMn_z)O_2$ hollow fibers with low cation mixing as high-performance cathode materials for Li-Ion batteries. Advanced Science, 2017, 4(1): 1600262(1-8). DOI: 10.1002/advs.201600262.

[3] Seidlmayer S, Buchberger I, Reiner M, et al. First-cycle defect evolution of $Li_{1-x}Ni_{1/3}Mn_{1/3}Co_{1/3}O_2$ lithium ion battery electrodes investigated by positron annihilation spectroscopy. Journal of Power Sources, 2016, 336: 224-230. DOI: 10.1016/j.jpowsour.2016.10.050.

[4] Otoyama M, Ito Y, Hayashi A, et al. Raman spectroscopy for $LiNi_{1/3}Mn_{1/3}Co_{1/3}O_2$ composite positive electrodes in all-solid-state lithium batteries. Electrochemistry, 2016, 84 (10): 812-814. DOI: 10.5796/electrochemistry.84.812.

[5] Hoang K, Johannes M. Defect physics and chemistry in layered mixed transition metal oxide cathode materials: (Ni, Co, Mn) vs (Ni, Co, Al). Chemistry of Materials, 2016, 28(5): 1325-1334. DOI: 10.1021/acs.chemmater.5b04219.

[6] Koyama Y, Arai H, Tanaka I, et al. Defect chemistry in layered $LiMO_2$ (M = Co, Ni, Mn, and $Li_{1/3}Mn_{2/3}$) by first-principles calculations. Chemistry of Materials, 2012, 24 (20): 3886-3894, DOI: 10.1021/Cm3018314.

[7] Vadlamani B, An K, Jagannathan M, et al. An in-situ electrochemical cell for neutron diffraction studies of phase transitions in small volume electrodes of li-ion batteries. J. Electrochem. Soc., 2014, 161 (10): A1731-A1741. DOI: 10.1149/2.0951410jes.

[8] Yan P F, Zheng J M, Lv D P, et al. Atomic-resolution visualization of distinctive chemical mixing behavior of Ni, Co, and Mn with Li in layered lithium transition-metal oxide cathode materials. Chemistry of Materials, 2015, 27 (15): 5393-5401. DOI: 10.1021/acs.chemmater.5b02016.

[9] Kitamura N, Ishida N, Idemoto Y. Atomic-configuration analysis on $LiNi_{0.5}Mn_{0.5}O_2$ by reverse monte carlo simulation. Electrochemistry, 2016, 84 (10): 789-792. DOI: 10.5796/electrochemistry.84.789.

[10] Zheng J X, Liu T C, Hu Z X, et al. Tuning of thermal stability in layered $Li(Ni_xMn_yCo_z)O_2$. Journal of the American Chemical Society, 2016, 138 (40): 13326-13334. DOI: 10.1021/jacs.6b07771.

[11] Koyama Y, Tanaka I, Adachi H, et al. Crystal and electronic structures of superstructural $Li_{1-x}[Co_{1/3}Ni_{1/3}Mn_{1/3}]O_2$ ($0 \leqslant x \leqslant 1$). Journal of Power Sources, 2003, 119-121: 644-648. DOI: 10.1016/S0378-7753(03)00194-0.

[12] Yabuuchi N, Koyama Y, Nakayama N, et al. Solid-state chemistry and electrochemistry of $LiCo_{1/3}Ni_{1/3}Mn_{1/3}O_2$ for advanced lithium-ion batteries. Journal of the Electrochemical Society, 2005, 152 (7): A1434-A1440. DOI: 10.1149/1.1924227.

[13] Yoon W S, Grey C P, Balasubramanian M, et al. Combined NMR and XAS study on local environments and electronic structures of electrochemically Li-ion deintercalated $Li_{1-x}Co_{1/3}Ni_{1/3}Mn_{1/3}O_2$ electrode system. Electrochemical and Solid-State Letters, 2004, 7 (3): A53-A55. DOI: 10.1149/1.1643592.

[14] Cahill L S, Yin S C, Samoson A, et al. ^{6}Li NMR studies of cation disorder and transition metal ordering in $Li[Ni_{1/3}Mn_{1/3}Co_{1/3}]O_2$ using ultrafast magic angle spinning. Chemistry of Materials, 2005, 17 (26): 6560-6566. DOI: 10.1021/cm0508773.

[15] Nedoseykina T, Kim S S, Nitta Y. Local atomic characterization of $LiCo_{1/3}Ni_{1/3}Mn_{1/3}O_2$ cathode material. Electrochim Acta, 2006, 52 (4): 1467-1471. DOI: 10.1016/j.electacta.2006.02.047.

[16] Stoyanova R, Ivanova S, Zhecheva E, et al. Correlations between lithium local structure and electrochemistry of layered $LiCo_{1-2x}Ni_xMn_xO_2$ oxides: ^{7}Li MAS NMR and EPR studies. Phys. Chem. Chem. Phys., 2014, 16 (6): 2499-2507. DOI: 10.1039/C3cp54438a.

[17] Gotoh K, Izuka M, Arai J, et al. In situ ^{7}Li nuclear magnetic resonance study of the relaxation effect in practical lithium ion batteries. Carbon, 2014, 79: 380-387. DOI: 10.1016/j.carbon.2014.07.080.

[18] Whitfield P S, Davidson I J, Cranswick L M D, et al. Investigation of possible superstructure and cation disorder

in the lithium battery cathode material $LiMn_{1/3}N_{1/3}Co_{1/3}O_2$ using neutron and anomalous dispersion powder diffraction. Solid State Ionics, 2005, 176 (5-6): 463-471. DOI: 10.1016/j.ssi.2004.07.066.

[19] Pang W K, Alam M, Peterson V K, et al. Structural evolution of electrodes in the NCR and CGR cathode-containing commercial lithium-ion batteries cycled between 3.0 and 4.5 V: An operando neutron powder-diffraction study. Journal of Materials Research, 2015, 30 (3): 373-380. DOI: 10.1557/jmr.2014.297.

[20] Levi E, Aurbach D. Crystal chemistry and valence determinations for Mn, Ni and Co oxides as cathode materials in Li batteries. Solid State Ionics, 2014, 257: 1-8. DOI: 10.1016/j.ssi.2014.01.024.

[21] Dolotko O, Senyshyn A, Muhlbauer M J, et al. Understanding structural changes in NMC Li-ion cells by in situ neutron diffraction. Journal of Power Sources, 2014, 255: 197-203. DOI: 10.1016/j.jpowsour.2014.01.010.

[22] Cherkashinin G, Ensling D, Jaegermann W. $LiMO_2$ (M = Ni, Co) thin film cathode materials: a correlation between the valence state of transition metals and the electrochemical properties. Journal of Materials Chemistry A, 2014, 2 (10): 3571 - 3580. DOI: 10. 1039/C3ta14509c.

[23] Yang C Z, Xie D C, Chen G Z, et al. Diffraction Analysis of Phases. Beijing: Metallurgic Industry Press, 1989.179-184.

[24] Levi E, Aurbach D. Lattice strains in the layered Mn, Ni and Co oxides as cathode materials in Li and Na batteries. Solid State Ionics, 2014, 264: 54-68. DOI: 10.1016/j.ssi.2014.06.020.